BMB
reports

Replication origins ori*GNAI3* and ori*B* of the mammalian *AMPD2* locus nested in a region of straight DNA flanked by intrinsically bent DNA sites

Valério Américo Balani[1], Quirino Alves de Lima Neto[1], Karen Izumi Takeda[1], Fabrícia Gimenes[1], Adriana Fiorini[1], Michelle Debatisse[2] & Maria Aparecida Fernandez[1,]*

[1]Departamento de Biologia Celular e Genética, Universidade Estadual de Maringá, UEM, Av. Colombo, 5790, 87020-900, Maringá, Paraná, Brasil, [2]Institut Curie, UMR 3244, 26 rue d'Ulm, 75248, Paris, France

The aim of this work was to determine whether intrinsically bent DNA sites are present at, or close to, the mammalian replication origins ori*GNAI3* and ori*B* in the Chinese hamster *AMPD2* locus. Using an electrophoretic mobility shift assay and *in silico* analysis, we located four intrinsically bent DNA sites (b1 to b4) in a fragment that contains the ori*GNAI3* and one site (b5) proximal to ori*B*. The helical parameters show that each bent DNA site is curved in a left-handed superhelical writhe. A 2D projection of 3D fragment trajectories revealed that ori*GNAI3* is located in a relatively straight segment flanked by bent sites b1 and b2, which map in previously identified Scaffold/Matrix Attachment Region. Sites b3 and b4 are located approximately 2 kb downstream and force the fragment into a strong closed loop structure. The b5 site is also located in an S/MAR that is found just downstream of ori*B*. [BMB reports 2010; 43(11): 744-749]

INTRODUCTION

Aside from its canonical double-helical structure, DNA is capable of forming conformational motifs such as hairpin, cruciform and curved structures (1). A curved DNA segment is formed by several main axis deflections of the double helix and is known as bent DNA. Bent DNA can be caused by flexibility at protein binding sites where the double helix warps when in contact with a binding partner (2, 3). A bent region may also be intrinsic, i.e., dependent on a nucleotide sequence comprising periodic repetitions of two or more adenine or thymine bases phased approximately every 10 base pairs (bp) or multiples of 10 bp (1, 4). The relationship between curved DNA segments and nuclear processes such as transcription, recombination and initiation at replication origins is an exciting research field. Our lab has been dedicated to mapping intrinsically bent DNA sites within genomic elements, e.g., promoters, replication origins, segments involved in recombination events and Scaffold/Matrix Attachment Regions, S/MARs (5-12). Now we are mapping these curved elements for the *AMPD2* amplified locus where seven replication origins were recently confirmed and mapped using the molecular combing methodology (13-15). Two of these replication origins, ori*GNAI3* and ori*B*, lie in well-studied segments and co-localize with previously described S/MARs (16). Our objective was to map intrinsically bent DNA sites on ori*GNAI3* and ori*B* segments by *in silico* and electrophoretic mobility shift analyses as well as 2D projections of 3D fragment trajectories. The results showed that intrinsically bent DNA sites, exhibiting left-handed superhelical writhe, are present near these two origins of the *AMPD2* locus.

*Corresponding author. Tel: 55-44-3011-1314; Fax: 55-44-3011-4893; E-mail: mafernandez@uem.br; aparecidafernandez@gmail.com
DOI 10.5483/BMBRep.2010.43.11.744

Received 2 September 2010, Accepted 29 September 2010

Keywords: Electrophoretic mobility shift assay, *In silico* analysis, Intrinsically bent DNA sites, Mammalian amplified *AMPD2* locus, ori*GNAI3* and ori*B* replication origins

RESULTS AND DISCUSSION

ENDS RATIO analysis of the amplified *AMPD2* locus

A large region of the *AMPD2* amplified locus (~65 kb), which contains ori*GNAI3*, ori*C*, ori*B* and ori*A*, was subjected to in silico analysis by using Map15 software to characterize the helical parameter for DNA curvature, ENDS ratio, Fig. 1. Several ENDS ratio peaks were observed and distributed throughout the entire segment, including near the replication origins (Fig. 1, gray boxes). However, in the regions of large replication initiation events (black boxes), no important peaks of ENDS ratio were observed. This scenario could indicate that intrinsically bent DNA sites only flank the replication origins. These sites could be responsible for building a 3D structure of these segments. To investigate this hypothesis, the helical parameters and electrophoretic mobility shift assay of ori*GNAI3* and ori*B* were analyzed.

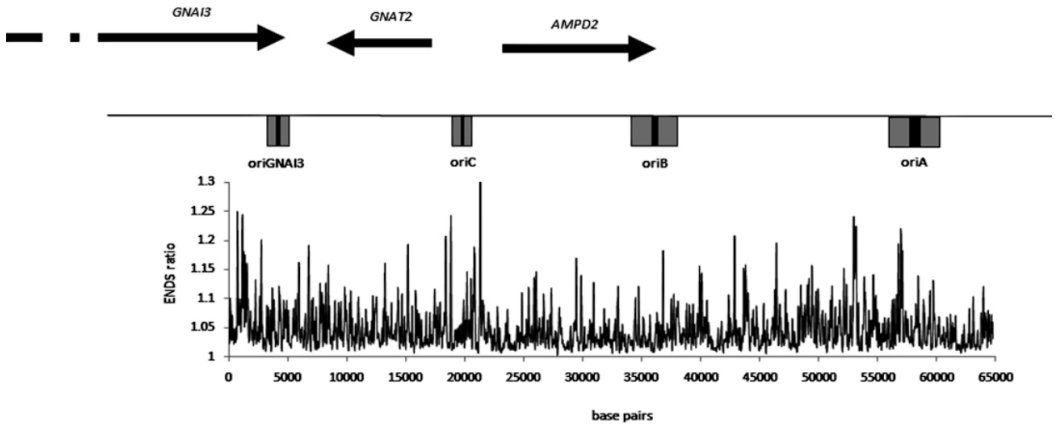

Fig. 1. *ENDS* ratio analysis of the Chinese hamster amplified *AMPD2* polygenic locus. The transcription directions of the *GNAI3*, *GNAT2* and *AMPD2* genes are showed by arrows on top. The gray boxes indicate the localization of the replication origins ori*GNAI3*, ori*C*, ori*B* and ori*A*, and the black area is the region where a large number of replication events take place (13).

The ori*GNAI3* and ori*B* segments contain intrinsically bent DNA sites of left-handed superhelical writhe

The 4.4 kb fragment harboring ori*GNAI3* displays four prominent peaks at nucleotide positions 570, 1,140, 2,830 and 3,660 bp with ENDS ratio values of 1.11 (b1), 1.12 (b2), 1.16 (b3) and 1.19 (b4), respectively (Fig. 2A). Only one pronounced peak with an ENDS ratio of 1.18 (b5) is observed at position 1,150 bp in the 2.5 kb segment that contains ori*B* (Fig. 2D). The helical parameters roll and twist angle were also analyzed. These parameters were selected for analysis given that intrinsically bent sites are known to exhibit negative Roll values, a decrease in the minor groove angle and Twist angles greater than 34.00°. Such features reveal curved, left-handed, superhelical DNA, which has been implicated in the binding of replication and transcription-associated proteins (17). In the 4.4 kb segment, all the intrinsically bent DNA sites display negative roll angles (−0.73; −0.25; −0.76 and −0.26; Fig. 2B) and twist angles greater than 34.00° (34.30°; 34.02°; 34.31° and 34.13°; Fig. 2C). The results reveal a curved and negative supercoiling DNA in these intrinsically bent DNA regions that are located upstream and downstream of ori*GNAI3*.

The 2.5 kb segment featured presents with a strong negative roll value of −1.1 (Fig. 2E) at the b5 location and a twist angle of 34.21° (Fig. 2F), indicating that the DNA at this site has a strong curved, left-handed superhelical writhe just downstream of ori*B*.

In silico analysis suggested that the putative intrinsically bent DNA sites are present in the environment of ori*GNAI3* and ori*B*. A mobility shift assay was performed to confirm these results.

Electrophoretic mobility shift assay confirms the presence of intrinsically bent DNA sites adjacent to IRs

Shifts of restriction fragments from the 4.4 kb and the 2.5 kb segments that respectively overlap ori*GNAI3* and ori*B* are shown in Fig. 3A and B. Only the *AvaI*/*BlnI* 1,516 bp fragment from the 4.4 kb segment, which contains the b3 and b4 bent DNA sites, exhibited retardation of its electrophoretic mobility in polyacrylamide (PA) gels (Fig. 3A, PA gel, lane 1, white arrowhead; R-value 1.15). The 2023 bp SacI/AvaI fragment, which contains the intrinsically bent DNA b1 and b2, migrated faster through the PA gel, yielding an R-value of approximately 0.90. Such electrophoretic behavior is indicative of non-centered bent DNA sites (5, 18). Indeed, the b1 and b2 sites lie in the initial third part of the fragment. None of the fragments stemming from the *PstI*/*AvaI* digestion (lane 2) showed strong retardation or faster migration. The 2D modeling analysis suggested that straight or curved fragments with segments in inverted orientation are responsible for the results (see Fig. 4A).

All fragments from the 2.5 kb region, which contains ori*B*, migrated quickly through the gel (Fig. 3B, PA gel, lanes 1 and 2, white arrowhead; R-values 0.84 and 0.83). The observed increase in mobility indicates the presence of bent DNA sites in one or both extremities (5, 18). Taking into account the position of restriction sites in the region, site b5 was difficult to centralize in a fragment and was instead assayed by circular permutation. The supplementary Fig. 1A shows detailed analysis of the ori*B* fragment by circular permutation. A 320 bp fragment (position 1,072 to 1,391 bp) containing the b5 site was amplified and cloned into the pBendBlue polylinker plasmid (19). The recombinant plasmid pBendBlue yields a 454 bp fragment, which comprises the 320 bp fragment, 13 bp from the pTZ plasmid which was derived from a previous cloning strategy and 121 bp from the pBendBlue polylinker. The plasmid was serially digested with *Bgl*II, *Xho*I, *Pvu*II, *Nru*I and *Kpn*I restriction enzymes. The fragment containing ori*B* has an AT rich S/MAR region, making it difficult to amplify a fragment

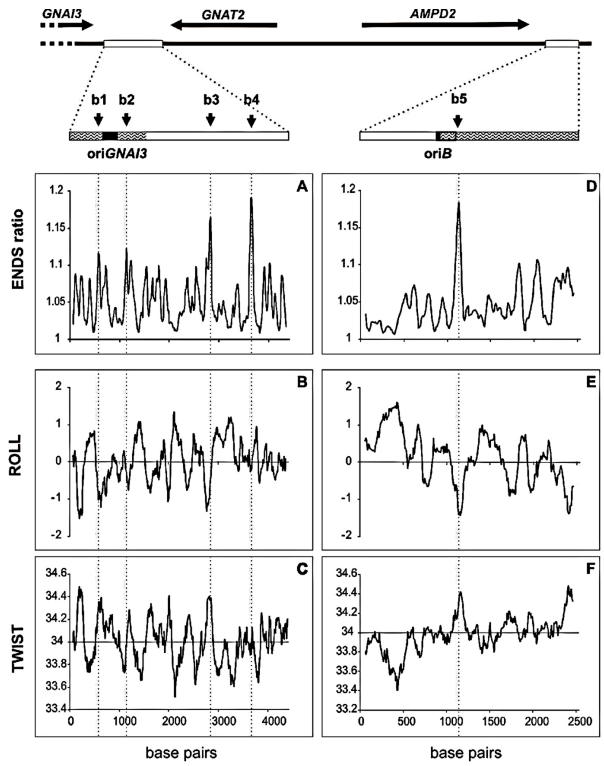

Fig. 2. *In silico* analysis of the replication origins ori*GNAI3* and ori*B*. A restriction map of the *AMPD2* amplified segment is shown in the diagram at the top of the figure, and the black horizontal arrows below the diagram indicate the direction of gene transcription. The wavy lines show the S/MARs (16) and the black bars show the location of the ori*GNAI3* and ori*B* IRs as previously described (14, 27). The vertical arrows indicate the ENDS ratio (A and D) of the prominent peaks and putative bent DNA sites in the 4.4 fragment, peak b1 (position 570), b2 (position 1140), b3 (position 2830), b4 (position 3660), and in the clone 2.5: peak b5 (position 1150). Among all sites, b1, b3 and b5 exhibited the lowest roll angle values, -0.73; -0.76; -1. (B and E) and the highest twist angles, 34.30°; 34.31°; 34.21°, respectively (C and F). The ENDS ratio, roll, and twist angle helical parameters were calculated within a 120 bp window and a 10 bp step employing Map15a software.

smaller than 320 bp. Nevertheless, the serial digestions confirmed the presence of the b5 intrinsically bent DNA site, which was also supported by the 2D model depicted (supplementary Fig. 1A and B).

As a control, the electrophoretic mobility shift assays described above were also conducted in the presence of ethidium bromide (EtBr), a DNA intercalating agent that abolishes curvature. When the fragments were assayed under these conditions, they migrated to positions in the gel concordant with their molecular sizes (data not shown).

2D structure and sequence analysis

The extent of the AT rich region and the 2D projection of the 3D trajectories of the 4.4 and 2.5 kb restriction fragments, which contain the intrinsically bent DNA sites, are shown in Fig. 4A and B, respectively. Although the AT rich region does not overlap with the intrinsically bent DNA sites, these sites are dependent on nucleotide periodicity, and the AT rich region must be considered when evaluating fragment stability. Fig. 4A and B show that all the intrinsically bent DNA sites studied here lay within sequences that are at least 55% AT rich. A complex structure is observed for the 4.4 kb segment (Fig. 4A) in which ori*GNAI3* is contained in a nearly straight segment, which is flanked by the b1 and b2 sites. Sites b3 and b4 drive the fragment in a closed loop structure, and all *in silico* attempts to extend this fragment using the 3D15m1 software failed. The bent DNA site b5 causes a change in the direction of the 2.5 kb fragment, and the 2D model also places ori*B* in a rigid, straight segment (Fig. 4B).

The 150 nucleotides surrounding each intrinsically bent DNA site in the amplified *AMPD2* domain were studied (supplementary Fig. 2). All observed intrinsically bent DNA sites presented with two or more Adenine or Thymine tracts, with a periodicity of 10 bp, or multiples of 10 bp (underlined). Sites b4 and b5 also harbor the CA_nT motif (double underline) described by Ohyama (17) as a motif that drives a sequence's curvature. Dinucleotide repeats (DNR), as described for the *DHFR* oriβ (20), are not found in the segments analyzed here for ori*GNAI3* and ori*B*.

The data presented here raise an interesting question: does the ori*GNAI3* structure favor access to the DNA for the replication machinery? In the eukaryotic nucleus, linear DNA is topologically constrained in a loop-organized fashion and the mechanisms of origin recognition could be closely associated with the chromatin structure. Recently, it was reported that the asymmetric pattern of the phased nucleosomes flanking the *Saccharomyces cerevisae* ACS, the consensus sequence of the ARS (autonomously replicating sequence), is important for the origin selection and function (21). The authors suggest that ORC-bound nucleosome-free-regions (NFRs) are flanked by nucleosomes positioned at precise intervals. In the *Drosophila* Kc167 cell line, approximately 5000 NFRs were reported, where the ORC complex is found to be associated. When analyzing the entire genome, the density of ORC binding could be associated with the replication timing in these cells (22). Intrinsically bent DNA sites, which could be responsible for distributing the nucleosomes in perfect phased segments, are the signal to the ORC complex binding in the NFR site? The intrinsically bent DNA sites b1 and b2 that flank ori*GNAI3* could explain the fact that this replication origin is the preferential site in the *AMPD2* amplified domain replication. The analysis of the nucleosome positioning in the segment that contains the ori*GNAI3* replication origin could provide evidence of the involvement of the intrinsically bent sites in *AMPD2* amplified segment replication initiation.

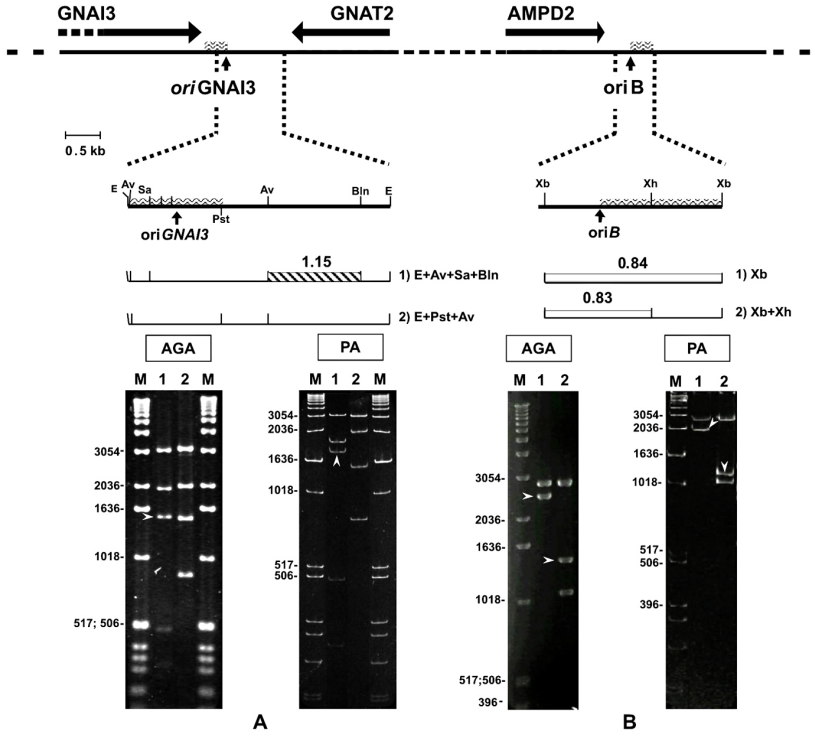

Fig. 3 Electrophoretic mobility shift assays of the ori*GNAI3* and ori*B* replication origins. A restriction map of the *AMPD2* amplified segment is shown in the diagram at the top of the figure. The black horizontal arrows below the diagram indicate the direction of gene transcription, the wavy lines demarcate S/MARs (16), and the horizontal black arrows indicate the location of ori*GNAI3* and ori*B* as previously described (14, 27). The restriction map at left shows the restriction fragments of the 4.4 kb clone that contains the ori*GNAI3* IR after digestion with *Eco*RI (E) + *Sac*I (Sa) + *Ava*I (Av) + *Bln*I (Bln) and *Eco*RI (E) + *Pst*I (Pst) + *Ava*I (Av) restriction enzymes, lanes 1 and 2, respectively. An *R*-value of 1.15 was observed for the *Ava*I + *Bln*I restriction fragment (white arrow in the gels), noted above the schematic representation of the same fragment (hatched bar). The restriction map at right shows the fragments obtained from the 2.5 kb clone that contains ori*B* after digestion with *Xba*I (Xb) and *Xba*I (Xb) + *Xho*I (Xh) restriction enzymes, lanes 1 and 2, respectively. The restriction fragments, with R-values of 0.84 and 0.85 are indicated in the gels and represented in the restriction map, above the gel figures. The other fragments didn't yield values smaller than 0.90 or above 1.10. M, 1 kb DNA ladder (Invitrogen); AGA, 1.0% agarose gel; PA, 6.0% polyacrylamide gels without ethidium bromide. The plasmid fragment had a migration close to the 3,054 bp position of the DNA ladder.

In conclusion, the results shown here describe the mapping and the helical parameters of intrinsically bent DNA sites in ori*GNAI3* and ori*B*. Further analysis is necessary to determine whether these structural features are involved in replication initiation of the *AMPD2* domain.

MATERIALS AND METHODS

Restriction fragments

The DNA under analysis is derived from the *AMPD2* amplified segment, which contains the genes *GNAI3, GNAT2*, *AMPD2* and *GSTM*. The ori*GNAI3* was identified in the intergenic region between the *GNAI3* and *GNAT2* genes and ori*B* in the *AMPD2* 3' segment (13, 23). The p4.4 kb plasmid (Y08232.1) that contains the intergenic region *GNAI3-GNAT2* and the p2.5 kb (X96547) plasmid that contains the 3' segment of the *AMPD2* gene were purified by the CTAB method (24) and cleaved with restriction endonucleases according to the manufacturer's instructions.

Electrophoretic mobility shift assay

The restriction fragments were examined in an electrophoretic mobility shift assay by first resolving them in a 1% agarose gel running at 3.5 V/cm at room temperature and through a 6% polyacrylamide (PA) gel at 7 V/cm at 4°C. The electrophoresis buffer was 1X TBE (45 mM Tris-borate, 1 mM EDTA, pH 8.0), and the gels were stained after electrophoresis with 1 μg/ml of EtBr and photographed under UV light (UVP BioImaging Systems). A 1 kb ladder (Invitrogen) was used as a molecular weight marker. An R-value, corresponding to the ratio of the observed fragment length to the real length, was calculated for each DNA fragment to determine the gel retardation. R-values between 0.90 and 1.09 signify no alteration in the fragment mobility; R-values greater than 1.10 indicate a reduced mobility, whereas R-values less than 0.90 signify an increase in mobility over what is expected for a given molecular size (25). The circular permutation experiments were performed for bent DNA site b5 as described elsewhere (7, 11, 12, 26). A 320 bp fragment (1,072 to 1,391 bp positions) was amplified with the following primers: forward 5'-TGC CCA GCG TTT CTC AGT GC-3' and reverse 5'-ACT CCT GGA GCA CCA GCC AG- 3' and cloned into the pTZ57R/T vector (InsTAclone PCR Cloning kit). A positive pTZ b5 clone was digested with *Xba*I and *Sal*I restriction enzymes and cloned into corresponding sites in the pBendBlue plasmid (19).

In silico analysis

In silico DNA curvature analyses of the sequences were carried out using Trifonov's wedge model (27). The 2D projection of the 3D trajectories was obtained with 3D15m1 software using the algorithm of Eckdahl and Anderson (28). The helical parameters were calculated using Map15a software as described elsewhere (11).

The *AMPD2* amplified locus and the restriction fragments of

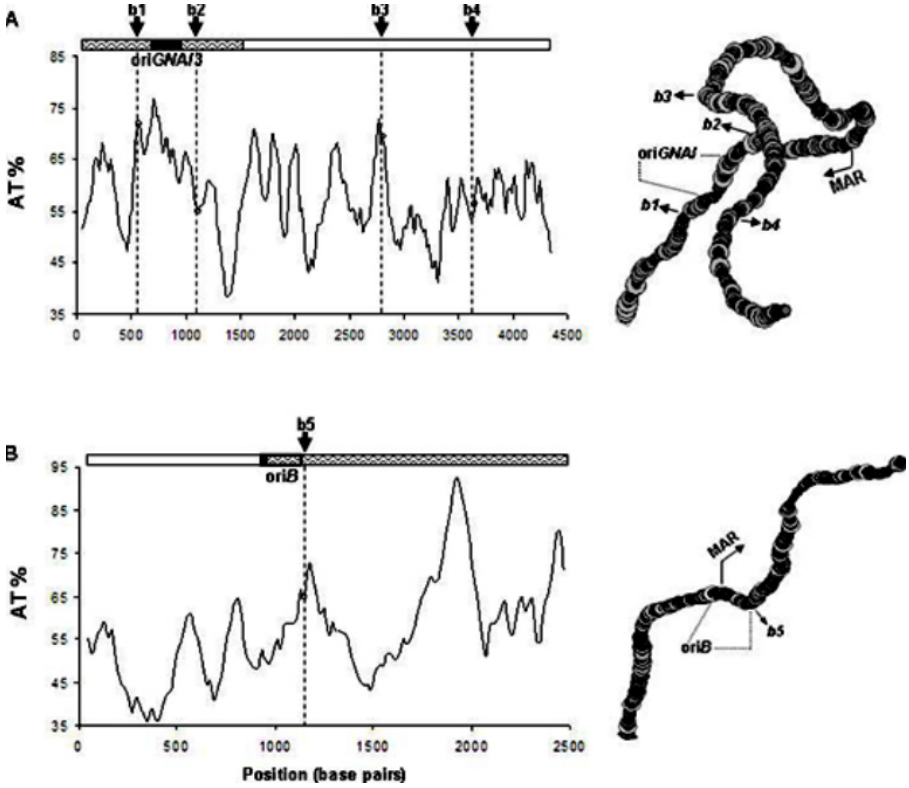

Fig. 4. Adenine/Thymine (AT) percentage and 2D projection of the 3D trajectories of the ori*GNAI3* and ori*B* regions. The 4.4 clone sequence containing the four intrinsically bent DNA sites b1, b2, b3 and b4 shows AT values higher than 50% with the highest AT values, 70 and 64%, in sites b1 and b3, respectively (A). The 2D projection shows that the ori*GNAI3* region has a nearly straight segment, only disturbed for a minor deflection caused by a short ENDS ratio peak at the right side of the b1 site (see Fig. 1). In this figure, it is clear that the intrinsically bent DNA site b3 is responsible for a change of the fragment direction. The 2.5 clone containing the oriB and the intrinsically bent DNA site b5 exhibits 68% AT, lower than observed for the MAR region, where a peak with almost 95% is present (B). Otherwise, the ori*B* segment 2D projection shows a more rigid straight DNA structure. There is a change in the direction of the fragment at the b5 site similar to what is seen at site b3. The wavy lines indicate the location of the S/MARs within the fragments.

the p4.4 and p2.5 clones were analyzed in a 120 bp window width and a 10 bp step for determination of the ENDS ratio (the ratio of the contour length of a fragment helical axis to the shortest distance between the fragment ends), twist angle (horizontal rotation among two consecutive base pairs), variations of the roll angle (which estimates the rolling-open of the base pairs along their long axes) and AT percentage.

Acknowledgements
We thank Valmir Peron and Marli Licero Schuete Silva for their dedicated technical assistance. This work was supported by grants from CNPq and The Academy of Sciences for the Developing World-TWAS and Universidade Estadual de Maringá facilities (COMCAP laboratories).

REFERENCES

1. Calladine, C. R., Drew, H. R., Luisi, B. F. and Travers, A. A. (2004) *Understanding DNA:* the *molecule and how it works,* 3nd ed., Elsevier Academic Press, Italy.
2. Zhang, Y., Xi, Z., Hegde, R. S., Shakked, Z. and Crothers, D. M. (2004) Predicting indirect readout effects in protein-DNA interactions. *Proc. Natl. Acad. Sci. U.S.A.* **101**, 8337-8341.
3. Bates, A., D. and Maxwell, A. (2005) *DNA Topology*. Oxford University Press, Oxford.
4. Anderson, J. N. (1986) Detection, sequence patterns and function of unusual DNA structures. *Nucleic. Acids. Res.* **14**, 8513-8533.
5. Fiorini, A., Basso, L. R. Jr., Paço-Larson, M. L. and Fernandez, M. A. (2001) Mapping of intrinsic bent DNA sites in the upstream region of DNA puff BhC4-1 amplified gene. *J. Cell Biochem.* **83**, 1-13.
6. Fiorini, A., Gouveia, F. S., Soares, M. A. M., Stocker, A. J., Ciferri, R. R. and Fernandez, M. A. (2006) DNA bending in the replication zone of the C3 DNA puff amplicon of Rhynchosciara americana (Diptera: Sciaridae). *Mol. Biol. Rep.* **33**, 71-82.
7. Fiorini, A., Gouveia, F. S. and Fernandez, M. A. (2006) Scaffold/Matrix Attachment Regions and Intrinsic DNA Curvature. *Biochemistry Mosc.* **71**, 481-488.
8. Barbosa, J. F., Bravo, J. P., Takeda, K. I., Zanatta, D. B., Silva, J. L. C., Balani, V. A., Fiorini, A. and Fernandez, M. A. (2008) Intrinsic bent DNA colocalizes with the sequence involved in the Nd-sD mutation in the Bombyx mori fibroin light chain gene. *BMB Rep.* **41**, 394-399.
9. Gouveia, F. S., Gimenes, F., Fiorini, A. and Fernandez, M. A. (2008) Intrinsic bent DNA sites in the developmentally amplified C3-22 gene promoter of Rhynchosciara americana (Diptera: Sciaridae). *Biosci. Biotechnol. Biochem.* **72**, 1190-1198.
10. Gimenes, F., Gouveia Fde, S., Fiorini, A. and Fernandez, M. A. (2008) Intrinsic bent DNA sites in the chromosomal replication origin of Xylella fastidiosa 9a5c. *Braz. J. Med.*

Biol. Res. **41**, 295-304.
11. Gimenes, F., Takeda, K. I., Gouveia, F. S., Fiorini, A. and Fernandez, M. A. (2008) Intrinsically bent DNA in replication origins and gene promoters. *Genet. Mol. Res.* **7**, 549-558.
12. Gimenes, F., Assis, M. A., Fiorini, A., Mareze, V. A. and Fernandez, M. A. (2009) Intrinsically bent DNA sites in the *Drosophila* melanogaster third chromosome amplified domain. *Mol. Genet. Genomics.* **281**, 539-549.
13. Anglana, M., Apiou, F., Bensimon, A. and Debatisse, M. (2003) Dynamics of DNA replication in mammalian somatic cells: nucleotide pool modulates origin choice and interorigin spacing. *Cell* **114**, 385-394.
14. Debatisse, M., Toledo, F. and Anglana, M. (2004) Replication initiation in mammalian cells: changing preferences. *Cell Cycle* **3**, 19-21.
15. Courbet, S., Gay, S., Arnoult, N., Wronka, G., Anglana, M., Brison, O. and Debatisse, M. (2008). Replication fork movement sets chromatin loop size and origin choice in mammalian cells. *Nature* **455**, 557-560.
16. Fernandez, M. A., Baron, B., Prigent, M., Toledo, F., Buttin, G. and Debatisse, M. (1997) Matrix attachment regions and transcription units in a polygenic mammalian locus overlapping two isochores. *J. Cell Biochem.* **67**, 541-551.
17. Ohyama, T. (2005) DNA conformation and transcription. Springer Science + Bussiness Media, New York, USA.
18. Wu, H., M. and Crothers, D. M. (1984) The locus of sequence-directed and protein-induced DNA bending. *Nature* **308**, 509-513.
19. Sperbeck, S. J. and Wistow, G. J. (1998) pBendBlue: modification of the pBend system for color selectability. *Biotechniques* **24**, 66-68.
20. Gray, S. J., Liu, G., Altman A. L., Small L. E. and Fanning E. (2007) Discrete functional elements required for initiation activity of the chinese hamster dihydrofolate reductase origin beta at ectopic chromosomal sites. *Exp. Cell Res.* **313**, 109-120.
21. Eaton, M. L., Galani, K., Kang, S., Bell, S. P. and MacAlpine, D. M. (2010) Conserved nucleosome positioning defines replication origins. *Genes. Dev.* **24**, 748- 753.
22. MacAlpine, H. K., Gordan, R., Powell, S. K., Hartemink, A. J. and MacAlpine, D. M. (2010) *Drosophila* ORC localizes to open chromatin and marks sites of cohesin complex loading. *Genome. Res.* **20**, 201-211.
23. Toledo, F., Baron, B., Fernandez, M. A., Lachages, A. M., Mayau, V., Buttin, G. and Debatisse, M. (1998) oriGNAI3: a narrow zone of preferential replication initiation in mammalian cells identified by 2D gel and competitive PCR replicon mapping techniques. *Nucleic. Acids. Res.* **26**, 2313-2321.
24. Del Sal, G., ManWoletti, G. and Schneider, C. (1989) The CTAB-DNA précipitation method: a common mini-scale preparation of template DNA from phagemids, phages or plasmids suitable for sequencing. *Biotechniques* **7**, 514-520.
25. de Souza, O. N. and Ornstein, R. L. (1998) Inherent DNA curvature and flexibility correlate with TATA box functionality. *Biopolymers* **46**, 403-415.
26. Kim, J., Zwieb, C., Wu, C. and Adhya, S. (1989) Bending of DNA by gene regulatory proteins: construction and use of a DNA bending vector. *Gene* **85**, 15-23.
27. Bolshoy, A., Mcnamaera, P., Harrington, R. E. and Trifonov, E. N. (1991) Curved DNA without A-A: experimental estimation of all 16 DNA wedge angles. *Proc. Natl. Acad. Sci. U.S.A.* **88**, 2312-2316.
28. Eckdahl, T. T. and Anderson, J. N. (1987) Computer modelling of DNA structures involved in chromosome maintenance. *Nucleic. Acids. Res.* **15**, 8531-8545.